ERS-TD: An Efficient Reconstruction and Sampling Method for TDOM Based on 3D Point Cloud Geometry in Image Cloud Computing

Jianyin Tang[1,2], Mingyu Lin[2], Zhenglin Yu[1], Zhenhua Xiao[2], Neal N. Xiong[3]*

[1] School of Mechanical and Electrical Engineering, Changchun University of Science and Technology, China
[2] School of Computer Science and Technology, Hubei Business College, China
[3] Department of Computer, Mathematical and Physical Sciences, Sul Ross State University, USA
tjyharry@hbc.edu.cn, linmingyu@hbc.edu.cn, yuzhenglin@cust.edu.cn, xiaozh@hbc.edu.cn, neal.xiong@sulross.edu

Abstract

Digital Orthophoto Map (DOM), as a crucial surveying and mapping product, often encounters issues such as occlusion, ghosting, and edge blur in practical applications, which undoubtedly have a negative impact on the accuracy of image analysis. The introduction of True Digital Orthophoto Map (TDOM) aims to effectively address these challenges, with its core objective being to eliminate interferences caused by terrain and ground target projection distortions. However, traditional TDOM production methods rely on digital surface models for orthorectification, a process that often results in the occlusion of high-rise buildings in the imagery due to the displacement of image points. In view of this, this paper proposes an Efficient Reconstruction and Sampling Method for TDOM Based on 3D Point Cloud Geometry in Image Cloud Computing (ERS-TD). This method innovatively integrates key technical components such as point cloud registration, absolute orientation, equal interval sampling, vertical projection, and texture mapping. Among these, the design of the equal interval sampling method is particularly ingenious, as it aims to efficiently and accurately extract surface point cloud data from the model. By flexibly adjusting the grid size of the sampling interval and comprehensively traversing the entire matrix, this method can rapidly and precisely obtain the surface point cloud information of the entire model, significantly improving efficiency compared to traditional methods. Furthermore, the vertical projection method projects the surface point cloud onto a plane, effectively eliminating the influence of elevation values and clearly revealing the outlines of buildings. In addition, to meet the demand for 3D map construction, this study further explores how to utilize the acquired 3D point cloud data and texture information to construct more refined and realistic 3D maps on the basis of generating True Digital Orthophoto Maps. By optimizing the processing flow of point cloud data and enhancing the accuracy of texture mapping, this study successfully achieves the transition from 2D imagery to 3D maps, providing new ideas and methods for 3D map construction.

Keywords: Oblique photo grammetry, True digital orthophoto map, 3D point cloud geometry, Equal interval sampling, Extraction and reconstruction

1 Introduction

Digital Orthophoto Map (DOM) has the geometric accuracy and complete image features of topographic map. It has become an important basic surveying and mapping product. However, there are often some problems in DOM, such as occlusion, ghosting, edge blur and incomplete integration [1], which affect the error of image analysis and interpretation. True Digital Orthophoto Map (TDOM) eliminates the projection deformation of terrain and ground targets at the same time, and the buildings, trees and other ground objects in the image are corrected to the correct position without blocking other ground objects. TDOM not only has the geometric accuracy and influence characteristics of DOM, but also is rich in texture information. It can be used for plane measurement, and can also obtain the correct road and building boundaries to build a 3D building scene [2]. The following figure is the comparison between DOM and the TDOM of urban buildings. It can be seen that the side texture of buildings is eliminated in the TDOM of urban scene, the roof was restored to its true position.

With the development of oblique photography, large-scale, multi angle, high-definition, high-precision and omni-directional complex scene perception becomes possible [3]. At the same time, with the support of the development of UAV, satellite and other platforms, the flight platform carries multiple sensors to obtain ground object images and elevation textures, which is gradually convenient and fast, and then carries out homonymous image point matching, regional network joint adjustment, inclined image dense matching, dense point cloud generation, triangulation construction, texture mapping and editing through the data processing platform [4]. The data processing operation of photogrammetry principle can finally realize the construction of large-scale and refined 3D point cloud geometry.

3D point cloud geometry is the product of 3D modeling of oblique photography, which has more intuitive and real characteristics. Domestic scholars have also studied the process of generating TDOM from this model. Based on the 3D model of oblique photography, Gu et al. [5] pro-

*Corresponding Author: Zhenglin Yu; Email: yuzhenglin@cust.edu.cn
DOI: https://doi.org/10.70003/160792642026012701011

posed a large-scale 3D digital topographic mapping method based on tilt photography technology, which realizes the mapping of large-scale 3D digital topographic maps; X. Zhu [6] and others used real 3D data to complete the production of TDOM through the acquisition of top view image data, the acquisition of control point information and the correction of image data; Guan et al. [7] completed the generation of TDOM by 3D reconstruction of scene model and sampling and pixels of the model. As shown in Figure 1, a comparison of the difference between the DOM and TDOM for urban buildings is presented.

Figure 1. Comparison of difference between DOM and TDOM of urban buildings

This paper studies the key technologies of TDOM production based on 3D point cloud geometry, including equal interval sampling and vertical projection of 3D point cloud geometry [8-10]. Experiments on multiple groups of data prove the practicability of this algorithm, which provides support for TDOM production and 3D data processing using 3D model [11-12].

This paper proposes a 3D map extraction and reconstruction scheme for image cloud computing. The paper is organized as follows: Section 2 provides an overview of related literature. Section 3 explains the methodology and data sources used. Section 4 presents our proposed scheme and compares it with existing methods. Section 5 provides a performance analysis. Finally, Section 6 concludes the paper and suggests future research directions.

2 The Related Work

In recent years, significant progress has been made in the fields of True Digital Orthophoto Map (TDOM) generation and 3D point cloud geometry applications, leading to the emergence of a series of innovative methods and applications. This section focuses on the relevant research work in this field, systematically summarizes the existing achievements, and lays a solid foundation for the research in this paper.

2.1 Research on Point Cloud Map Representation and Applications

Point cloud maps, due to their rich 3D scene information, have been widely used in multiple fields. With the development of sensor technology and the improvement of algorithms, research on the generation and application of point cloud maps has continued to deepen. Lee et al. [13] developed a coarse-to-fine method, consisting of the Building Exterior Wall-Based (BEWB) algorithm and the Building Outline-Based (BOB) algorithm, to register point clouds captured by different sensors in urban scenes. Specifically, the BEWB algorithm performs coarse registration of urban point clouds by extracting building exterior walls, establishing corresponding points, and effectively removing outliers from the corresponding point set. In contrast, the BOB algorithm achieves precise registration of urban point clouds acquired from multiple sensors by leveraging building outlines and points corresponding to the point cloud ground. by Chiang et al. [14] explored the application of point cloud maps in autonomous vehicle navigation. By constructing a real-time point cloud processing algorithm, vehicles can accurately perceive the surrounding environment and achieve safe and reliable path planning. This achievement provides a new direction for the development of the intelligent transportation field and also offers new ideas for the application of TDOM in urban traffic modeling.

In addition, with the development of computer vision technology, some studies have attempted to use deep learning methods for semantic understanding of 3D point cloud data [15-17]. These methods can automatically identify different ground object categories in the point cloud, improving the analysis efficiency and accuracy of point cloud data and providing powerful tools for information extraction and classification of TDOM.

2.2 Research on Data Acquisition Technologies

Data acquisition is a key link in obtaining high-quality point cloud data, and certain progress has been made in mobile laser scanning and airborne multi-spectral laser scanning.

In the field of mobile laser scanning, Antero Kukko et al. [18] have developed multi-platform mobile laser scanning solutions (such as vehicle-mounted, cart-mounted, and boat-mounted devices) for data acquisition in urban areas and river environments. They have also launched a new type of backpack-mounted device, which is suitable for measurement needs in the field of natural sciences under variable terrain conditions, and discussed the application performance of these solutions in various fields including urban surveying and mapping, river geomorphology, etc.. At the same time, significant progress has also been made in UAV-based laser scanning technology [19]. UAV laser scanning can obtain high-resolution point cloud data from a low-altitude perspective, making it possible to finely map urban and natural environments.

In airborne multi-spectral laser scanning, K. Bakuła et al. [20] used advanced multi-spectral airborne laser scanning equipment combined with deep learning algorithms to achieve high-precision classification of land cover types. This research improves the semantic information acquisition ability of point cloud data, provides a more accurate basis for ground object classification and information extraction of TDOM, and expands the application value of TDOM. In addition, some studies have explored the fusion

methods of multi-spectral laser scanning data with other data sources [21-22], improving the recognition and classification accuracy of complex ground objects by comprehensively utilizing different types of data.

2.3 Research on TDOM Generation

TDOM generation has always been a research focus in the fields of photogrammetry and remote sensing, and many scholars have carried out research from different perspectives. Wei et al. [23] proposed TDOM-NeRF, a novel large-scale urban True Digital Orthophoto Map (TDOM) generation method based on Neural Radiance Fields (NeRF). This method does not rely on additional prior information; instead, it takes multi-view Unmanned Aerial Vehicle (UAV) images as input and employs hash grid features and a Multi-Layer Perceptron (MLP) to implicitly represent the scene. By performing orthogonal volume rendering on the scene reconstruction results, the problem of uneven scales of synthesized views during TDOM generation is effectively solved. In practical training, a scene block training strategy is adopted to extend the method to TDOM generation for large-scale scenes, while achieving high-fidelity scene reconstruction. Qu et al. [24] proposed a novel image-to-image method that can directly generate high-quality True Digital Orthophoto Maps (TDOMs) from multi-view satellite images without the need for elevation data as input. Specifically, the 3D scene is effectively represented by volumetric density and color, both of which are modeled using a neural network. During each iteration, this 3D representation is optimized via multi-view satellite signals, with the adoption of a volumetric rendering formula. Finally, the TDOM is generated using the orthogonal volumetric rendering technique. In addition, some studies have focused on quality control and evaluation methods during the TDOM generation process [25-26]. These methods establish a scientific evaluation index system to comprehensively evaluate the accuracy, completeness, and consistency of TDOM, providing a guarantee for improving the quality of TDOM.

3 Our Proposed ERS-TD

In the in-depth exploration of the production technology of True Digital Orthophoto Maps (TDOM) and the geometric applications of 3D point clouds, to address the problems existing in traditional methods, this paper proposes an Efficient Reconstruction and Sampling method for TDOM based on 3D Point Cloud Geometry in Image Cloud Computing (ERS-TD). This method integrates multiple key technologies, covering multiple links from data processing to TDOM generation and 3D map construction. The following will elaborate on its key components such as the system model, core algorithms, and processes in detail.

3.1 System Model and Key Definitions

In the process of generating TDOM based on 3D point cloud geometry, a series of important technical steps and concepts are involved. Clarifying these contents is crucial for understanding and implementing the ERS-TD method.

In indoor mapping scenarios, point cloud data acquired by some measurement technologies that do not rely on the Global Navigation Satellite System (GNSS) lack georeferencing information, which can easily lead to deviations between different datasets. To address this issue, Rönnholm proposed 13 orientation methods, among which the 3D surface matching method has attracted much attention. This method can generate large-area multi-source data by registering non-georeferenced datasets with large georeferenced “blocks”. In addition, airborne laser scanning (ALS) data can assist in improving the registration effect of the mobile laser scanning (MLS) system, as the visibility of GNSS signals in different areas for the MLS system varies. In practical operations, precise registration is the foundation for subsequent work, ensuring that point cloud data from different sources can be fused and processed in a unified geographic coordinate system.

The density distribution of point cloud data acquired by laser scanning is not uniform, and this non-uniformity can have adverse effects on subsequent modeling and other applications. The purpose of down-sampling technology is to generate a uniform point cloud density by reducing redundant data close to the scanner. Before performing down-sampling, it is necessary to identify overlapping areas in the data and quantify them based on density. Then, sampling is carried out on the overlapping data to generate a single, uniform point cloud. For example, when scanning complex buildings, the point cloud close to the scanner may be too dense. Down-sampling can reduce the data volume while retaining key information and improve processing efficiency.

Data integration is an important process of incorporating multiple types of information into point cloud data to enhance its application value. Point clouds are essentially a record of the environment at a specific moment. Incorporating temporal information into point clouds can enhance their ability to express environmental changes. By combining temporal information with point data, data filtering in the temporal dimension can be achieved. For example, when monitoring urban construction progress, the latest point cloud information can be extracted from scanning data at different times, or point cloud pairs can be generated to detect changes in objects such as buildings. The incorporation of temporal information provides strong support for analyzing the dynamic changes of the environment.

The accuracy of point clouds is closely related to the sensors used in the acquisition process. To better meet the requirements of different applications for data accuracy, it is crucial to add accuracy information to the point cloud, preferably in the form of global position accuracy. In this way, accuracy standards can be set according to specific needs in practical applications, and the reliability of the data can be evaluated. When higher-accuracy point data is available, lower-accuracy points can be excluded in a timely manner to achieve intelligent data updating. For example, in high-precision urban terrain mapping, accurate accuracy information can help surveyors accurately judge the usability of the data.

Point clouds usually contain spectral information obtained through sensor integration or laser backscatter intensity and waveform analysis. Incorporating these spectral data during the analysis and segmentation of point clouds can significantly improve the accuracy of the results, especially when using multi-spectral sensors. Spectral information can provide additional basis for distinguishing different types of ground objects, such as distinguishing vegetation from buildings. By analyzing spectral data, the features of ground objects can be extracted more accurately, and the classification accuracy of point cloud data can be improved.

Accurate point cloud classification and segmentation are the basis for extracting object parameters and building object models. When each point in the point cloud is assigned a label describing the object it represents (such as "building", "tree", etc.), the point cloud becomes a semantic point cloud. After segmenting the point cloud, assigning specific identifiers (such as national building identifiers) to all points belonging to the corresponding buildings can further enrich the semantic information of the point cloud. This semantic information plays an important role in visualization and analysis applications. For example, in urban environment analysis, specific types of ground object points can be quickly screened out through semantic information, such as excluding vegetation points and focusing on the analysis of artificial ground objects like buildings and roads.

3.2 Point Cloud Denoising and Classification Algorithm

The original point cloud data contains a large amount of noise, which can result in excessive data size, and the original point cloud is not effectively classified, leading to low efficiency in subsequent processing. Therefore, this paper proposes a denoising and classification algorithm based on the original point cloud to preprocess it before further processing.

3.2.1 Improved Point Cloud Denoising Algorithm Based on Statistical Features

The original point cloud data collected by UAV has a large amount of data with a lot of noise, which needs to be de-noised. The noise points can be divided into the following four types through analysis.

- The drift noise points: Sparse or scattered points at the edge of the principal point cloud, away from the principal point cloud;
- The isolated noise points: away from the principal point cloud, the small and dense noise point set;
- The redundancy noise points: extra scan points beyond the predetermined range;
- The mixed noise points: miscellaneous points intermingled with the principal point cloud.

Due to the complexity of point cloud data noise, an improved point cloud denoising algorithm based on statistical features is proposed in this paper. The principle is that the average distance between each point in the model data set containing point cloud and its domain conforms to the Gaussian distribution, and the statistical analysis method of the average distance in the local domain of the point cloud is compared with the principal point cloud, and the noise point is denoised [27-30].

First, assume that the number of points in the noise point cloud model P is n, the k-field point set of any point pi is N(Pi). The average distance di between any point pi in the point cloud and all adjacent points in the k-field can be used to calculate through the Equation (1). Then, the average distance d0 of the all local fields is obtained as show in Equation (2), σ is the standard deviation of the average distance in the local field of point cloud, as shown in Equation (3). When the k-field average distance di>d_0+λσ, pi will be removed as noise.

$$d_i = \frac{1}{k}\sum_{j=1}^{k}\left|p_j - p_i\right|, p_j \in N(p_i) \tag{1}$$

$$d_0 = \frac{1}{N}\sum_{i=1}^{N} d_i \tag{2}$$

$$\sigma = \sqrt{\frac{1}{n}\sum_{i=1}^{N}\left(d_i - d_0\right)^2} \tag{3}$$

When the k-field average distance di >d0+λσ, pi will be removed as noise.

3.2.2 Point Cloud Data Classification Processing Based on Feature Vector Stochastic Forest Classification Algorithm

The denoising point cloud data contains vegetation, buildings, terrain, vehicles and other point cloud data, and this paper needs to extract the terrain point cloud. In order to extract the terrain point cloud, the point cloud data should be effectively classified, and the terrain point cloud should be extracted after classification.

The geometric features of point cloud can effectively distinguish vegetation, buildings, terrain, vehicles and other information. Seven feature vectors can be obtained through the linear, planar and three-dimensional attributes of the point and its field. The obtained feature vectors are poured into the random forest classification algorithm for the classification of point cloud data.

With the current point as the center, the nearest k points are searched to form a adjacent points set P={p1, …, pi, …, pk}, then the covariance tensor C_X is shown in in Equation (4).

$$C_X = \frac{1}{k}\sum_{i=1}^{k}\left(p_i - \hat{p}\right)\left(p_i - p\right)^T \tag{4}$$

Where, $\hat{p}$ is the center point of *k*-field points, the calculation Equation (5) is shown below:

$$\hat{p} = \arg\min_p \sum_{1}^{k}\left\|p_i - \sum_{i=1}^{k} p_i\right\| \tag{5}$$

As shown in Equation (5), we seek a point $\hat{p}$ in space such that the sum of the squared distances from it to all

points in the neighboring point set p is minimized. This point a can be regarded as the "central" position of the neighboring point set p in space. Accurately determining point $\hat{p}$ is crucial for the subsequent precise calculation of the covariance tensor and the construction of feature vectors, as it can better describe the geometric characteristics of the point cloud data in the local region and provide a more reliable basis for point cloud data classification.

In the process of point cloud data classification using the eigenvector-based random forest classification algorithm, the three eigenvalues λ1, λ2, and λ3 are typically computed using eigenvalue decomposition. For a 3×3 covariance tensor C_X, its eigenvalue decomposition is given by Equation (6):

$$C_X = U\Lambda U^T \tag{6}$$

Where U is an orthogonal matrix composed of eigenvectors, and Λ is a diagonal matrix with the eigenvalues λ1, λ2, and λ3 on its diagonal. In practical computations, various mathematical libraries (such as the NumPy library in Python) can be employed to perform this process. By applying eigenvalue decomposition to the covariance tensor C_X, we can obtain three eigenvalues that satisfy λ1> λ2>λ3>0. Subsequently, seven feature vectors are constructed based on these eigenvalues for the classification of point cloud data. These seven feature vectors can be derived from the three eigenvalues, as shown in Table 1.

Table 1. Seven feature vectors constructed based on feature values

Eigenvector	Size
Linearity	$V_1 = (\lambda_1 - \lambda_2)/\lambda_1$
Plananrity	$V_2 = (\lambda_2 - \lambda_3)/\lambda_1$
Seatter	$V_3 = \lambda_3/\lambda_1$
Anisotropy	$V_4 = (\lambda_1 - \lambda_3)/\lambda_1$
Eigenentropy	$V_5 = -\sum_{i=1}^{3} \lambda_i \times \ln(\lambda_i)$
Omnivariance	$V_6 = \sqrt[3]{(\lambda_1 \times \lambda_2 \times \lambda_3)}$
Surface variation	$V_7 = \lambda_3$

In this paper, the random forest algorithm is used to classify the point cloud data. The feature vector consists of seven groups of feature vectors constructed by three eigenvalues. After training, the overall classification accuracy is about 85%.

3.3 TDOM Production Process

The existing mature digital photogrammetry systems include Pixel Factory, INPHO, etc. these digital photogrammetry systems have been able to produce TDOM with high precision. The processes of TDOM production by these systems are: digital aerial triangulation to DSM extraction, DSM editing, digital TDOM correction, splicing and color uniformity.

3.3.1 Production Process of Traditional TDOM

The traditional method of TDOM uses Digital Surface Model (DSM) and digital differential correction technology to correct the geometric deformation of the original image, so that every point on the image is corrected to the vertical angle of view. In reality, the fluctuation of the ground will cause the difference between the actual image position of the ground point and the ideal image position, resulting in the displacement of the image point. Image point displacement often leads to occlusion and ghosting of tall ground objects. As shown in Figure 2, orthophoto correction will produce image point displacement when the ground fluctuates greatly.

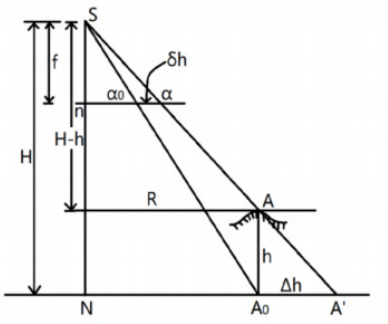

Figure 2. Schematic diagram of image point displacement during orthophoto correction

3.3.2 Production Process of TDOM

In this paper, the TDOM is made for the 3D point cloud geometry of oblique photography, and the 3D point cloud geometry obtained by 3D reconstruction of unmanned aerial photography image and high-resolution satellite image is experimentally processed. The TDOM generation steps in this paper are shown in Figure 3. The production from 3D point cloud geometry to TDOM is completed by performing point cloud registration and fusion, absolute orientation of model, interval sampling, vertical projection and texture mapping on the input model.

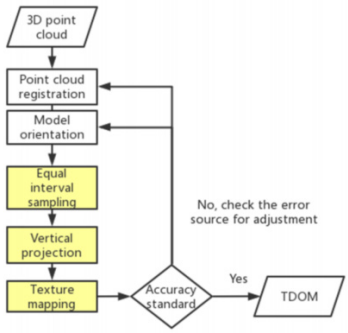

Figure 3. Information processing flow of TDOM generation system

Figure 3 illustrates the information processing flow of the TDOM generation system. Initially, three-dimensional point clouds serve as the input data. After undergoing

point cloud registration and model optimization, the data is sequentially subjected to equidistant sampling, vertical projection, and texture mapping operations.

Following the completion of texture mapping, the processing results must be compared against accuracy standards for evaluation. The specific accuracy standards are as follows:

Geometric Accuracy Standards: The mean error in planar position should not exceed ±0.5 meters (relative to the true ground coordinates), and the mean error in elevation should not exceed ±0.3 meters. These standards ensure that the TDOM accurately reflects the actual terrain and landforms in both planar position and elevation.

Image Resolution Standards: The spatial resolution of the image must reach 0.2 meters, meaning each pixel corresponds to an actual ground size of 0.2 meters × 0.2 meters. This ensures that the image details meet the application requirements.

Color Consistency Standards: In the overlapping areas of adjacent images, the standard deviation of color differences should not exceed 10 (calculated in the RGB color space). This ensures that the overall image has natural color transitions and consistent visual effects.

If the processing results meet the aforementioned accuracy standards, the TDOM is output. If not, the sources of error must be identified and corrected, after which the process returns to the point cloud registration step for reprocessing.

3.4 Equal Interval Sampling

Equal interval sampling is to extract the point cloud data on the surface of the point cloud geometry, cover the model in the form of a two-dimensional matrix with sufficient density, extract the highest point of the model of each small grid as the sample point in the grid area, and traverse the whole point cloud geometry to extract the surface point cloud of the model.

3.4.1 Principle of Equal Interval Sampling

This paper implements the equal interval sampling method, surrounds the space of the registered and oriented 3D point cloud geometry with a cube, establishes a two-dimensional matrix with M rows and N columns, divides the whole cube into square cubes with the same bottom size. By adjusting the size of the matrix cell network, the algorithm finds the point with the largest elevation value in the 3D point cloud geometry in the cube where each cell network is located as the sample point in the grid, and stores it in the point set. It traverses the whole matrix to obtain the surface point cloud of the whole model. If the extracted point set is sparse, it will reduce the size of the grid and traverse the whole model again, until the point cloud on the whole model surface is extracted. The schematic diagram of equal interval sampling is shown in Figure 4.

3.4.2 Algorithm Flow of Equal Interval Sampling

The flow of the algorithm is as follows:

1. Calculate the minimum and maximum values in X, Y and Z directions of the whole model, and record them as X min, X max, Ymin, Ymax and Zmin, Z max;

2. Calculate the difference between the maximum and minimum values in X and Y directions to obtain the length and width of the whole grid:

m = Xmax-Xmin

N=Ymax-Ymin

3. Set the side length of the cell net and the number of cells per unit length, then: cell=1/cell_length;

4. To calculate the number of cells in the whole large grid, it is necessary to round up and include the bottom of the whole model, including:

row = [m * cell]

col = [n * cell]

cellsum = row * col

Where the is the number of small cells in the entire grid, the is the number of small cells in the X direction and the is the number of small cells in the Y direction.

5. Traverse the whole grid, find the maximum value point of Z-axis in each small cell, record the index of the extreme point at this time, and store it in the index sequence, which is taken at the boundary of the grid;

$x \in [\ Xmin + i * cell\_length, Xmin + (i+1) * cell\_length\ ) \cup Xmin + row * cell\_length\ ]$

$i \in [\ Q \mid 0 \le i \le row\ ]$

$y \in [\ Ymin + j * cell\_length, Ymin + (j+1) * cell\_length\ ) \cup Ymin + row * cell\_length\ ]$

$j \in [\ Q \mid 0 \le j \le row\ ]$

6. Copy the point cloud recorded by the index and store it in a new point cloud set for display.

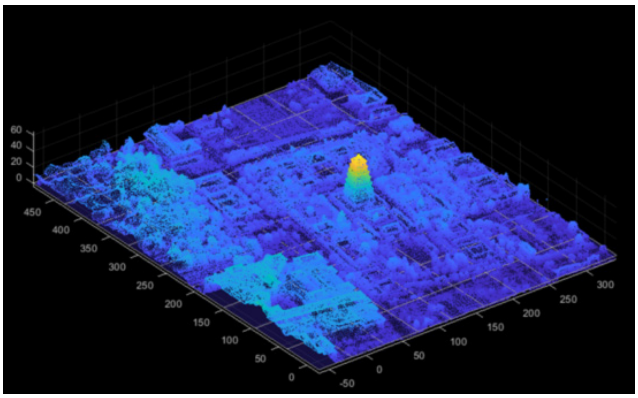

Figure 4. Schematic diagram of 3D point cloud geometry placed in equally spaced sampling grid

3.5 Vertical Projection

Vertical projection is the top view projection of orthographic projection, which has authenticity, accumulation and similarity. The large 3D scene model constructed by tilt photography objectively reproduces the omni-directional scene of the survey area. Based on the characteristics of vertical projection, the texture information corresponding to dense matching points or interpolation points in the top view can be extracted from the tilt photography scene model to generate true orthophoto images required by other projects.

Vertically project the plane position of the point set on the horizontal plane and form the corresponding plane graphics of the equally spaced sampling surface point cloud set. In this paper, the surface point cloud extracted by equal interval sampling vertically projects the xoy plane, as shown in Figure 5.

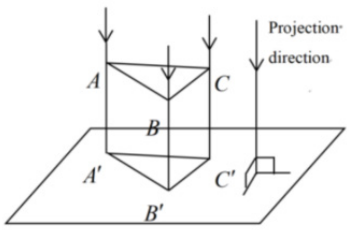

Figure 5. Schematic diagram of vertical projection

In this paper, the vertical projection adopts the projection method of parametric model provided in PCL, projectinliers filter, and the 3D point cloud sampled at equal intervals is filtered. The parametric setting of the model parameters modelcoefficients by the projectinliers filter can realize the projection operation of the point cloud geometry on the two-dimensional plane, line, sphere and cylinder.

The flow of vertical projection algorithm is as follows:

- Input the 3D point set after equal interval sampling, and record the start time of the algorithm;
- Set the four parameters of the parametric model. The plane model is. When setting the parameters, set a, B and D as 0 and C as 1 to construct a plane with Z = 0;
- The input model is filtered by projectinliers to obtain the vertical projection of the model;
- Store the point set after vertical projection, and calculate the time-consuming algorithm.

3.6 Algorithm

The following is the pseudo code for the generation of TDOM based on three-dimensional point cloud geometry in technical writing style.

The TDOM generation process involves uniform sampling and vertical projection of the input three-dimensional point cloud. The pseudo code for this process is shown in Algorithm 1.

Algorithm 1. TDOM algorithm

Input: inputPointCloud (point cloud data that needs to be processed)

Output: projectedPointCloud (point cloud data after being processed by the Uniform Sampling, Vertical Projection, and Return TDOM functions)

```
1. Function: Uniform Sampling
2. begin
3.    Xmin, Xmax, Ymin, Ymax, Zmin, Zmax = calculate MinMax(inputPointCloud)
4.    m = Xmax - Xmin
5.    n = Ymax - Ymin
6.    cell_length = calculateCellLength(inputPointCloud)
7.    row = round(m / cell_length)
8.    col = round(n / cell_length)
9.    cellsum = row * col
10.   indexList = []
11.   for i = 0 to row do
12.      for j = 0 to col do
13.         x_min = Xmin + i * cell_length
14.         x_max = Xmin + (i + 1) * cell_length
15.         y_min = Ymin + j * cell_length
16.         y_max = Ymin + (j + 1) * cell_length
17.      subPointCloud = extractSubPointCloud(inputPoint Cloud, x_min, x_max, y_min, y_max)
18.         maxZIndex = findMaxZIndex(subPointCloud)
19.         indexList.append(maxZIndex)
20.      end
21.   end
22.outputPointCloud=extractPointCloudByIndices(inputP ointCloud, indexList)
23.   // Function: Vertical Projection
24.   planeModel = setPlaneModel()
25.projectedPointCloud=projectPointCloudToPlane(outpu tPointCloud, planeModel)
26.   // Function: Return TDOM
27.   return projectedPointCloud
28. end
```

To generate TDOM, we first perform uniform sampling on the input three-dimensional point cloud to extract the surface point cloud of the model. The uniform sampling process involves dividing the point cloud into small grids and extracting the highest point in each grid. The extracted points are then used to generate the output point cloud.

Next, we perform vertical projection on the output point cloud to generate the TDOM. The vertical projection process involves projecting the point cloud onto a plane with Z=0. This is achieved by setting a plane model and using it to project the point cloud onto the plane.

Finally, the generated TDOM is returned as the output of the function.

4 Performance Analysis

4.1 Experimental Environment and Data Preparation

This paper uses C + + programming combined with PCL library to realize the function of 3D point cloud geometry processing. The experimental environment of this paper is shown in Table 2:

Table 2. Configuration of experimental environment

Name	Parameter
CPU	Intel(R) Core(TM) i7-8750H CPU @2.20GHz 2.21GH
GPU	GeForce RTX2070
Memory	32.0GB
Operating system	Microsoft Windows 10
Debugging environment	Microsoft Visual Studio 2017
Third party Library	PCL 1.9.0

To comprehensively verify the performance of the method proposed in this paper, experimental tests were conducted using a 3D point cloud geometric model generated from multi-view satellite images and a 3D real-scene model of the Big Wild Goose Pagoda in Xi'an captured by an unmanned aerial vehicle (UAV). The point cloud of the 3D point cloud geometric model from satellite images carries grayscale information, while the point cloud of the UAV 3D real-scene model has no color information, and its color texture is attached to the triangular mesh. The above data model is shown in Figure 6.

Name	Data presentation	Point cloud number
Some regional model of the Big Wild Goose Pagoda		477789
Complete model of the Big Wild Goose Pagoda		482032
Satellite reconstruction model in some region of South America		700854
Satellite reconstruction model in some region of South America		233530
Satellite Reconstruction Model in a certain region of South America-Perspective 1		1692601

Figure 6. Data model

4.2 Performance Analysis of Equal-Interval Sampling

4.2.1 Determination and Adjustment of Grid Size

The side length of the square grid is calculated and set based on the maximum and minimum values of the 3D point cloud geometric model after absolute orientation in the X, Y, and Z directions. When determining the grid size, both model complexity and processing efficiency need to be considered. If the grid is too large, the extracted point cloud will be sparse and unable to accurately represent the model surface; if the grid is too small, the computational load and processing time will increase. After multiple parameter adjustments, a reasonable grid size is found to ensure that the model is completely covered and the point cloud density is appropriate. When adjusting the grid size, it is found that different types of models have different sensitivities to grid size. For models with complex structures, a smaller grid is required to accurately capture their details; for relatively simple models, an overly large grid will lead to the loss of details, but an overly small grid will increase unnecessary computational load. In practical applications, the grid size needs to be dynamically adjusted according to the characteristics of the model and application requirements. For example, a smaller grid should be used when performing fine modeling of architectural models; when conducting rough modeling of regional terrain, the grid size can be appropriately increased.

4.2.2 Determination and Adjustment of Grid Size

In this experiment, the point cloud geometric model of the Big Wild Goose Pagoda in Xi'an reconstructed from UAV images was used, and the model was divided into grids with a side length of 1×1 cm pixels. From the experimental results shown in Figure 7 (Figure 7(a) displays the leveled data model of the original Big Wild Goose Pagoda model, represented by green point clouds; Figure 7(b) shows the point cloud data extracted using equal-interval sampling with a square grid size of 1×1 cm, represented by red point clouds), the extracted point clouds are dense and completely cover the model surface. This indicates that the equal-interval sampling algorithm can accurately extract the point clouds on the model surface. At this grid size, the details of the model are effectively preserved, such as the doors, windows, and eaves of the Big Wild Goose Pagoda, which are clearly visible. Further analysis reveals that the equal-interval sampling algorithm can well maintain the geometric features of objects with regular shapes; however, when dealing with some irregular shapes, such as natural objects like trees, it may lead to the loss of some details due to the limitations of sampling points. This is because equal-interval sampling is based on regular grids and has relatively weak adaptability to irregular shapes. In subsequent research, other sampling methods, such as feature-based sampling, can be considered to achieve more accurate sampling of objects with irregular shapes.

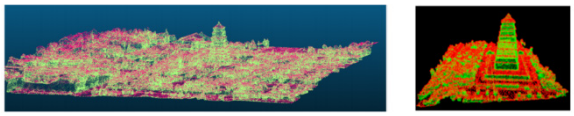

(a) (b)

Figure 7. Overall schematic diagram and local details of equal-interval sampling: (a) shows the leveled data model of the original Big Wild Goose Pagoda model (represented by green point clouds); (b) presents the point cloud data extracted via 1×1 cm square grid equal-interval sampling (represented by red point clouds)

4.2.3 Analysis of Equal-Interval Sampling Results from Satellite Images

Figure 8 presents a comparison between the original 3D point cloud geometric model from satellite images and the 3D point cloud geometric model after equal-interval sampling. Visually, after the original model undergoes equal-interval sampling processing, the side point cloud data are filtered out, while the surface data remain complete and clear. The figure shows the comparison of experimental results of equal-interval sampling from satellite images. The results indicate that the algorithm effectively removes redundant point clouds, retaining only the key surface information, which improves the efficiency and accuracy of subsequent processing. This verifies the effectiveness and applicability of the algorithm for processing 3D point cloud geometric models generated from satellite images. However, when processing satellite images, it is found that factors such as cloud cover can affect the sampling results. The point cloud data in the areas covered by clouds may be inaccurate, leading to missing or incorrect information in these areas after sampling. In practical applications, for the preprocessing of satellite images, in addition to conventional operations such as denoising, it is also necessary to add the identification and processing of areas covered by clouds. Image segmentation techniques can be used to first identify the cloud-covered areas, and then the point cloud data in these areas can be supplemented through interpolation or other data sources to improve the accuracy of the sampling results.

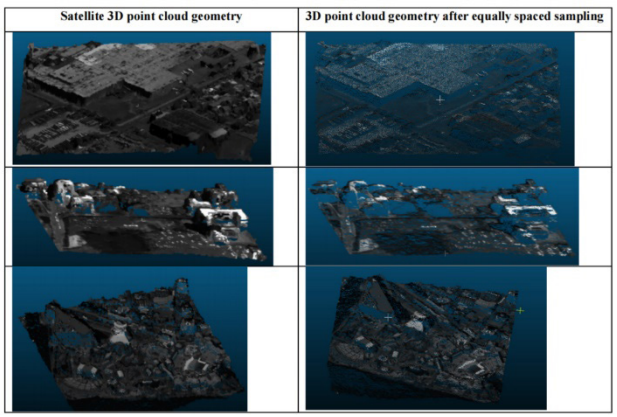

Figure 8. Comparison between original satellite 3D point cloud geometry and equidistant sampling 3D point cloud geometry

4.3 Performance Analysis of Vertical Projection

4.3.1 Vertical Projection Algorithm

The point cloud data obtained by equal-interval sampling is vertically projected onto the XOY plane. Using the projectInliers filter method in the PCL (Point Cloud Library), we set the plane parameters A = B = D = 0 and C = 1 to obtain the parameters for the plane model Z = 0. Then, the sampled point cloud is filtered, and the elevation value of the processed point cloud is set to 0 for visualization and display. When using the projection method in the PCL, it is found that different versions of the library have differences in projection accuracy and speed. Newer versions of the library may have optimized algorithms, improving projection accuracy, but may also increase the computational load due to added features, resulting in slower projection speeds. In practical applications, it is necessary to select an appropriate version of the library according to specific requirements. If high projection accuracy is required, a new version of the library can be chosen; if speed is a more critical factor, a more suitable version needs to be selected by comprehensively considering the functions and performance of the library.

4.3.2 Analysis of Vertical Projection Effects

The experimental results (combined with Figure 7(a), Figure 7(b) and Figure 9. [Figure 7(a) shows the point cloud after equal-interval sampling before vertical projection; Figure 7(b) shows the point cloud after vertical projection; Figure 9 shows the comparison between the model before vertical projection and the plane after vertical projection, presenting the overall and partial data of the Big Wild Goose Pagoda from both side and top-view perspectives]) indicate that vertical projection eliminates the elevation values of the point cloud. After projection, the surrounding features of the Big Wild Goose Pagoda are distinct, and the outlines of the houses are clear. The Z-axis data of the point cloud is eliminated after projection, the model remains complete, and the algorithm runs at a high speed. It effectively converts 3D point cloud data into 2D planar data, preserving key features and improving processing efficiency. However, during the projection process, it is found that when the point cloud data contains noise or the model surface is discontinuous, abnormal projection results may occur. For example, at the edges of some models, projection distortion may appear. This is because noise points and discontinuous surfaces can affect the projection algorithm's judgment of the model structure. In subsequent research, data preprocessing can be added before projection, such as more rigorous denoising or smoothing the model surface, to improve the quality of the projection results.

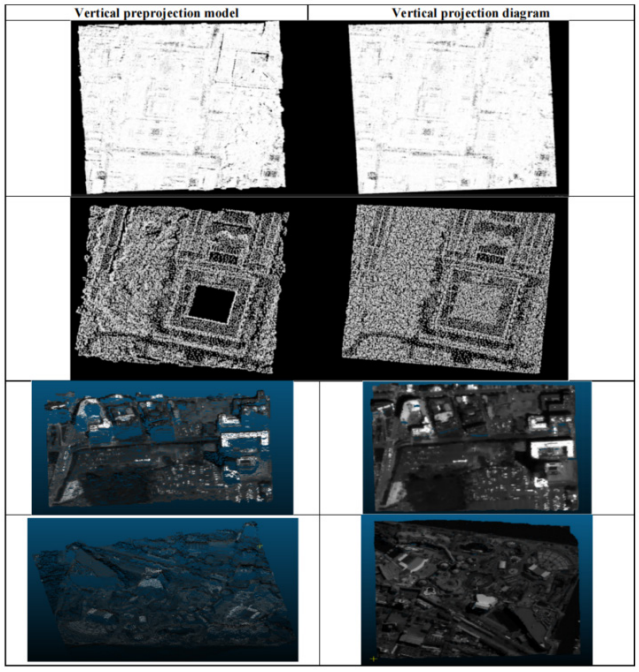

Figure 9. Comparison between model before vertical projection and plane after vertical projection

4.4 Performance Analysis of Texture Mapping

After vertical projection, texture mapping is carried out on the satellite-reconstructed point cloud with grayscale information to obtain Figure 10, which includes a grayscale effect image and a pseudo-color effect image. The grayscale effect image clearly displays the surface features of the model, while the pseudo-color effect image intuitively reflects different areas of the model through color variations. Texture mapping adds visual information to the True Digital Orthophoto Map (TDOM), enhancing its readability and practicality. However, during the texture mapping process, some areas have problems such as low texture fit, stretching, or distortion. These issues may be caused by factors such as the quality of the point cloud data and the accuracy of the texture mapping algorithm. Subsequent optimization of the algorithm is required to improve the texture fit. Further analysis reveals that the effect of texture mapping is also related to the density of the point cloud. When the point cloud density is low, texture mapping may appear blurry or discontinuous; when the point cloud density is too high, it will increase the computational load and processing time. In practical applications, appropriate texture mapping algorithms and parameters need to be selected according to the point cloud density and texture quality requirements. For example, for low-density point clouds, an interpolation-based texture mapping method

can be used to improve the continuity of the texture; for high-density point clouds, a more complex but more accurate algorithm can be employed to enhance the texture fit.

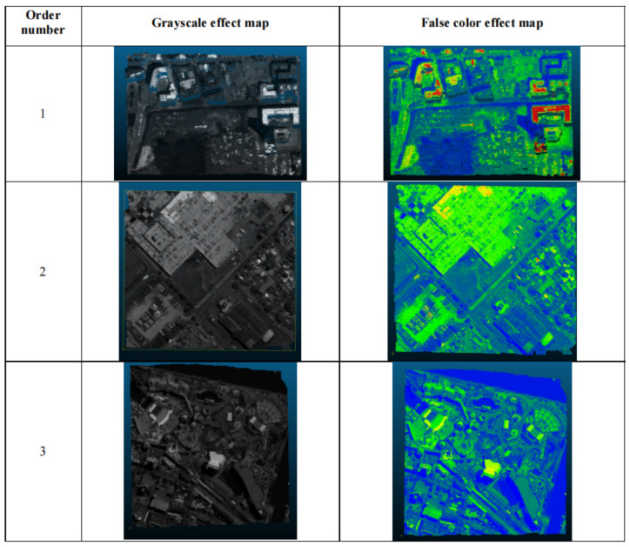

Figure 10. Effect picture of TDOM generated by 3D point cloud geometry of satellite image with gray scale

4.5 Comparative Analysis with Other Methods

Comparing our method with traditional TDOM production methods, the traditional methods are prone to problems such as occlusion and ghosting when dealing with complex scenes and large-scale point cloud data. Our method effectively eliminates these problems through equal-interval sampling and vertical projection, generating more accurate and clear TDOMs. In terms of algorithm efficiency, our method also has an advantage, as it can complete TDOM production in a relatively short time. However, compared with some emerging deep learning methods, our method is still lacking in automation. Deep learning methods can automatically learn the features and patterns of point cloud data through large-scale data training, enabling more intelligent TDOM production. Nevertheless, deep learning methods require a large amount of training data and strong computing resources, and the interpretability of the models is poor. In practical applications, the advantages of our method and deep learning methods can be combined to improve automation while ensuring algorithm efficiency and accuracy. For example, in the data preprocessing stage, our method can be used for rapid point cloud sampling and projection, and then the processed data can be used as input for the deep learning model. The powerful feature-learning ability of the deep learning model can be leveraged to further optimize the TDOM generation effect.

In summary, our TDOM production method based on 3D point cloud geometry has obvious performance advantages. It can effectively handle complex scenes and large-scale point cloud data to generate high-quality TDOMs. However, there are deficiencies in aspects such as texture mapping and automation, which require further research and improvement.

5 Conclusion

In this paper, the TDOM is made based on the 3D point cloud geometry, and the algorithm of equal interval sampling and vertical projection of the TDOM is studied. This part is the key to generate the TDOM. The TDOM can be used as the source of mapping, map vectorization and monomer modeling, which plays an important role in the future digital city, environmental monitoring and emergency response.

For the equal interval sampling of the 3D point cloud geometry, debug the size of the cell network at the sampling interval, extract the maximum elevation point of the point cloud data falling in each cell network as the sampling point of the cell network, and traverse the whole matrix to obtain the surface point cloud data of the whole model. This process depends on absolute orientation or model flattening algorithm. Only when the model is flattened, the equal interval sampling method in this paper is effective; The point cloud with elevation value obtained after equal interval sampling is vertically projected. The projection is based on XOY plane, and the surface point cloud obtained by equal interval sampling is brought into it for vertical projection. Projection results all points fall on the plane, all point clouds form a plane from the side view, and the building outline in the original model is also obvious from the top view.

The equal interval sampling method in this paper takes one minute to calculate the local wild goose pagoda model. When the amount of data increases, the calculation time increases exponentially. In the follow-up research, the sampling grid setting will be further improved. Through the estimation of the model edge, the calculation of blank cells will be reduced, and the algorithm will be accelerated to improve the efficiency of equal interval sampling in the case of large amount of data. Through the experiments of equal interval sampling and vertical projection, the TDOM of multi view satellite image is generated in this paper. Compared with the model, it can be seen that there are still some shadows and a small number of holes. It is further necessary to add this part of the image in the same area to make up for the problems caused by the lack of images or shadows.

Acknowledgements

This work was supported by the Project of Science and Technology Department of Jilin Province, China (Grant number: 202002044JC). It was also supported by the Natural Science Foundation of Hubei Province of China (Grant number: 2022CFB536). Jianyin Tang and Mingyu Lin contributed equally to this work.

References

[1] J. X. Yang, Z. L. Cai, T. J. Wang, T. Ye, H. R. Gao, H. Huang, Ortho-3DGS: True Digital Orthophoto Generation From Unmanned Aerial Vehicle Imagery Using the Depth-

Regulated 3D Gaussian Splatting, *IEEE Journal of Selected Topics in Applied Earth Observations and Remote Sensing*, Vol. 18, pp. 10972–10994, March 2025. https://doi.org/10.1109/JSTARS.2025.3552105

[2] X. Wang, W. Zhang, H. Xie, H. Ai, Q. Q. Yuan, Z. Q. Zhan, Tortho-Gaussian: Splatting True Digital Orthophoto Maps, https://arxiv.org/abs/2411.19594, November, 2024. https://doi.org/10.48550/arXiv.2411.19594

[3] N. G. Jiao, F. Wang, Y. X. Hu, Y. M. Xiang, R. Liu, H. J. You, SAR True Digital Ortho Map Production for Target Geometric Structure Preservation, *IEEE Journal of Selected Topics in Applied Earth Observations and Remote Sensing*, Vol. 16, pp. 10279–10286, October, 2023. https://doi.org/10.1109/JSTARS.2023.3328049

[4] Y. Zeng, C. J. Sreenan, L. Sitanayah, N. Xiong, J. H. Park, G. Zheng, An Emergency-Adaptive Routing Scheme for Wireless Sensor Networks for Building Fire Hazard Monitoring, *Sensors*, Vol. 11, No. 3, pp. 2899–2919, March, 2011. https://doi.org/10.3390/s110302899

[5] L. Gu, H. Zhang, X. J. Wu, Surveying and mapping of large-scale 3D digital topographic map based on oblique photography technology, *Journal of Radiation Research and Applied Sciences*, Vol. 17, No. 1, Article No. 100772, March, 2024. https://doi.org/10.1016/j.jrras.2023.100772

[6] X. Zhu, *The Study of the Real Projective Image Based on TDOM*, Master's Thesis, Chengdu University of Technology, Chengdu, Sichuan, China, 2018. https://kns.cnki.net/KCMS/detail/detail.aspx?dbname=CMFD201901&filename=1018259277.nh

[7] H. Guan, H. Jiang, T. Cao, X. Liu, Construct 3D models of scene on true orthoimage, *Science of Surveying and Mapping*, Vol. 34, No. 3, pp. 71–73, 2009. https://d.wanfangdata.com.cn/periodical/chkx200903025

[8] K. Chen, Y. Liu, J. Zhang, T. Zhang, K. Liu, J. Yang, GPRT: A Gaussian Process Regression-Based Radio Map Construction Method for Rugged Terrain, *IEEE Internet of Things Journal*, Vol. 12, No. 13, pp. 23905–23920, July, 2025. https://doi.org/10.1109/JIOT.2025.3554507

[9] P. E. Kuevor, M. Ghaffari, E. M. Atkins, J. W. Cutler, Fast and Noise-Resilient Magnetic Field Mapping on a Low-Cost UAV Using Gaussian Process Regression, *Sensors*, Vol. 23, No. 8, Article No. 3897, April, 2023. https://doi.org/10.3390/s23083897

[10] J. Yang, N. Xiong, A. V. Vasilakos, Z. Fang, D. Park, X. Xu, S. Yoon, S. Xie, Y. Yang, A Fingerprint Recognition Scheme Based on Assembling Invariant Moments for Cloud Computing Communications, *IEEE Systems Journal*, Vol. 5, No. 4, pp. 574–583, December, 2011. https://doi.org/10.1109/JSYST.2011.2165600

[11] S. Huang, Z. Zeng, K. Ota, M. Dong, T. Wang, N. N. Xiong, An Intelligent Collaboration Trust Interconnections System for Mobile Information Control in Ubiquitous 5G Networks, *IEEE Transactions on Network Science and Engineering*, Vol. 8, No. 1, pp. 347–365, January-March, 2021. https://doi.org/10.1109/TNSE.2020.3038454

[12] J. Yang, X. P. Li, L. Luo, L. W. Zhao, J. Wei, T. Ma, New Supplementary Photography Methods after the Anomalous of Ground Control Points in UAV Structure-from-Motion Photogrammetry, *Drones*, Vol. 6, No. 5, Article No. 105, May, 2022. https://doi.org/10.3390/drones6050105

[13] E. Lee, Y. Kwon, C. Kim, W. Choi, H. G. Sohn, Multi-source Point Cloud Registration for Urban Areas Using a Coarse-to-Fine Approach, *GIScience & Remote Sensing*, Vol. 61, No. 1, Article No. 2341557, 2024. https://doi.org/10.1080/15481603.2024.2341557

[14] K. W. Chiang, S. Srinara, Y. T. Chiu, S. Tsai, M. L. Tsai, C. Satirapod, N. El-Sheimy, M. Ai, Creation and Verification of High-Definition Point Cloud Maps for Autonomous Vehicle Navigation, *IEEE Internet of Things Journal*, Vol. 11, No. 23, pp. 37582–37598, December, 2024. https://doi.org/10.1109/JIOT.2024.3435344

[15] C. R. Qi, H. Su, K. Mo, L. J. Guibas, PointNet: Deep Learning on Point Sets for 3D Classification and Segmentation, *Proc. IEEE Conference on Computer Vision and Pattern Recognition*, Honolulu, HI, USA, pp. 77–85, 2017. https://doi.org/10.1109/CVPR.2017.16

[16] C. R. Qi, L. Yi, H. Su, L. J. Guibas, PointNet++: Deep Hierarchical Feature Learning on Point Sets in a Metric Space, *Proc. Advances in Neural Information Processing Systems*, Long Beach, CA, USA, pp. 5105–5114, 2017. https://dl.acm.org/doi/10.5555/3295222.3295263

[17] Y. Wang, Y. Sun, Z. Liu, S. E. Sarma, M. M. Bronstein, J. M. Solomon, Dynamic Graph CNN for Learning on Point Clouds, *ACM Transactions on Graphics (TOG)*, Vol. 38, No. 5, pp. 1–12, October, 2019. https://doi.org/10.1145/3326362

[18] A. Kukko, H. Kaartinen, J. Hyyppä, Y. Chen, Multiplatform Mobile Laser Scanning: Usability and Performance, *Sensors*, Vol. 12, No. 9, pp. 11712–11733, September, 2012. https://doi.org/10.3390/s120911712

[19] A. M. Almeshal, M. R. Alenezi, A. K. Alshatti, Accuracy Assessment of Small Unmanned Aerial Vehicle for Traffic Accident Photogrammetry in the Extreme Operating Conditions of Kuwait, *Information*, Vol. 11, No. 9, Article No. 442, September, 2020. https://doi.org/10.3390/info11090442

[20] K. Bakuła, P. Kupidura, Ł. Jełowicki, Testing of Land Cover Classification from Multispectral Airborne Laser Scanning Data, *The International Archives of the Photogrammetry, Remote Sensing and Spatial Information Sciences*, Vol. XLI-B7, pp. 161–169, 2016. https://doi.org/10.5194/isprs-archives-XLI-B7-161-2016

[21] G. Sohn, I. Dowman, Data fusion of high-resolution satellite imagery and LiDAR data for automatic building extraction, *ISPRS Journal of Photogrammetry and Remote Sensing*, Vol. 62, No. 1, pp. 43–63, May, 2007. https://doi.org/10.1016/j.isprsjprs.2007.01.001

[22] X. X. Zhu, D. Tuia, L. Mou, G. S. Xia, L. Zhang, F. Xu, F. Fraundorfer, Deep Learning in Remote Sensing: A Comprehensive Review and List of Resources, *IEEE Geoscience and Remote Sensing Magazine*, Vol. 5, No. 4, pp. 8–36, December, 2017. https://doi.org/10.1109/MGRS.2017.2762307

[23] J. X. Wei, G. B. Zhu, X. L. Chen, NeRF-Based Large-Scale Urban True Digital Orthophoto Map Generation Method, *IEEE Journal of Selected Topics in Applied Earth Observations and Remote Sensing*, Vol. 18, pp. 1070–1084, 2025. https://doi.org/10.1109/JSTARS.2024.3491869

[24] Y. J. Qu, X. Y. An, S. H. Chen, F. Deng, Satellite True Digital Orthophoto Map Generation Without Elevation Data: A New NeRF-Based Method, *Remote Sensing Letters*, Vol. 15, No. 3, pp. 258–269, 2024.

https://doi.org/10.1080/2150704X.2024.2313608

[25] Y. Imai, Y. Akamatsu, M. Mori, N. Shirai, M. Maruya, H. Ohyama, An Accuracy Assessment of DSMs and Orthoimages Derived from ALOS/PRISM and Their Availability in Forestry, *The International Archives of the Photogrammetry, Remote Sensing and Spatial Information Sciences*, Vol. XXXVII, Part B8, pp. 1021-1025, 2008.

[26] D. El-Rushaidat, R. Yeh, X. M. Tricoche, Accurate parallel reconstruction of unstructured datasets on rectilinear grids, *Journal of Visualization*, Vol. 24, No. 4, pp. 787–806, August, 2021.
https://doi.org/10.1007/s12650-020-00740-0

[27] X. Wu, J. Xu, Z. Zhu, Y. Wang, Q. Zhang, S. Tang, M. Liang, B. Cao, Correlation filter tracking algorithm based on spatial-temporal regularization and context awareness, *Applied Intelligence*, Vol. 52, No. 15, pp. 17772–17783, December, 2022.
https://doi.org/10.1007/s10489-022-03458-8

[28] Q. Wang, Q. H. Gu, L. Chen, Y. P. Guo, N. X. Xiong, A MOEA/D with global and local cooperative optimization for complicated bi-objective optimization problems, *Applied Soft Computing*, Vol. 137, Article No. 110162, April, 2023.
https://doi.org/10.1016/j.asoc.2023.110162

[29] Z. Feng, L. Yan, Y. Xia, B. Xiao, An Adaptive Padding Correlation Filter With Group Feature Fusion for Robust Visual Tracking, *IEEE/CAA Journal of Automatica Sinica*, Vol. 9, No. 10, pp. 1845–1860, October, 2022.
https://doi.org/10.1109/JAS.2022.105878

[30] K. Li, A Survey of Multi-objective Evolutionary Algorithm Based on Decomposition: Past and Future, *IEEE Transactions on Evolutionary Computation*, Early Access, pp. 1–1, 2024.
https://doi.org/10.1109/TEVC.2024.3496507

Biographies

Jianyin Tang is a PhD Candidate at Changchun University of Science and Technology. Currently, he is a Senior Engineer. His research interests include machine learning and machine vision.

Mingyu Lin is an M.S. graduate from Nanchang Hangkong University, China. Currently, she is an associate professor at the School of Computer Science and Technology, Hubei Business College, China. Her research interests include pattern recognition and data analysis.

Zhenglin Yu prof. & doctoral supervisor at Changchun Univ. of Sci. & Tech. (China), now works at its Mechatronic Eng. Dept. He researches mechatronic system control. Led projects like China's Nat. Nat. Sci. Found., covering deep hole inner-surface photoelectric detection and airborne photoelectric countermeasure platforms. Won Jilin Provincial & National Defense Sci-Tech Progress Awards, published papers (e.g., 3D Point Cloud Registration for Complex Surfaces via iGPS), and holds titles like Jilin's Middle-aged & Young Sci-Tech Leader.

Zhenhua Xiao is a Ph.D. in Computer Science. Currently, he is an associate professor. His research interests include artificial immune systems, image recognition, fault diagnosis, and IoT security.

Neal N. Xiong is a professor, holds dual PhDs from Japan's Graduate School of Frontier Sciences (Univ of Electro-Communications) and China's Wuhan Univ (Sch of Comp Sci); he teaches at Georgia State Univ (Dept of Comp Sci) and Colorado Sch of Mines (USA), was nominated for China Computer Federation's Excellent Doctoral Dissertation Award, and has published ~500 papers (≈250 journal ones) in venues like IEEE JSAC, IEEE/ACM Transactions, IEEE INFOCOM.